Proc. Natl. Acad. Sci. USA
Vol. 91, pp. 10024–10028, October 1994
Biophysics

Luminescence energy transfer using a terbium chelate: Improvements on fluorescence energy transfer

(lanthanide elements/europium/Förster theory/resonance)

PAUL R. SELVIN* AND JOHN E. HEARST

Department of Chemistry, University of California, and Structural Biology Division, Lawrence Berkeley Laboratory, Berkeley, CA 94720

Communicated by Ignacio Tinoco, June 15, 1994

ABSTRACT **We extend the technique of fluorescence resonance energy transfer (FRET) by introducing a luminescent terbium chelate as a donor and an organic dye, tetramethylrhodamine, as an acceptor. The results are consistent with a Förster theory of energy transfer, provided the appropriate parameters are used. The use of lanthanide donors, in general, and this pair, in particular, has many advantages over more conventional FRET pairs, which rely solely on organic dyes. The distance at which 50% energy transfer occurs is large, 65 Å; the donor lifetime is a single exponential and long (millisecond), making lifetime measurements facile and accurate. Uncertainty in the orientation factor, which creates uncertainty in measured distances, is minimized by the donor's multiple electronic transitions and long lifetime. The sensitized emission of the acceptor can be measured with little or no interfering background, yielding a >25-fold improvement in the signal-to-background ratio over standard donor–acceptor pairs. These improvements are expected to make distances >100 Å measurable via FRET. We also report measurement of the sensitized emission lifetime, a measurement that is completely insensitive to total concentration and incomplete labeling.**

Fluorescence resonance energy transfer (FRET), in which a fluorescent donor molecule transfers energy via a nonradiative dipole–dipole interaction to an acceptor molecule (which is usually a fluorescent molecule), is a standard spectroscopic technique for measuring distances in the 10- to 70-Å range. Upon energy transfer, which depends on R^{-6}, where R is the distance between the donor and acceptor, the donor's lifetime and quantum yield are reduced, and the acceptor fluorescence is increased, or sensitized (1). The technique is frequently used in both polymer science and structural biology and has recently been used to study macromolecular complexes of DNA, RNA, and proteins (2–4).

Despite these successes, FRET has a number of serious flaws that limit its utility. First, the maximum distance that can be measured is less than optimal for many biological applications. Second, the lifetimes of commonly used donor fluorophores are short (typically a few nanoseconds) and multiexponential, making lifetime measurements difficult and of limited accuracy. Third, the signal-to-background ratio of the sensitized emission is low due to interfering fluorescence from the donor and from direct excitation of the acceptor. Fourth, precise distances are difficult to determine because the efficiency of energy transfer depends not only on the R^{-6} distance between the donor and acceptors but also on their relative orientation, as expressed by the κ^2 factor. [The efficiency of energy transfer = $1/(1 + R^6/R_o^6)$, where R_o (the distance at which 50% energy transfer occurs) is a function of κ^2; see *Calculation of* R_o in *Appendix*].

The luminescent lanthanide elements terbium and europium are attractive FRET donors because they potentially overcome many of these problems. Because lanthanide emission does not arise from a singlet-to-singlet transition, energy transfer using lanthanide donors is more accurately called luminescence resonance energy transfer. The lanthanides have primarily been used in diffusion-enhanced FRET (5) and as isomorphous replacements in calcium-binding proteins (6–8). In addition, Mathis (9) has used europium cryptates with the multichromophoric allophycocyanin to achieve an extremely large R_o of 90 Å. We have recently presented results showing numerous advantages of using a polycarboxylate chelate of europium as a donor in conjunction with an organic dye such as CY-5 as the acceptor (10). Here we extend these results to the use of terbium as a donor.

As a model system, we covalently attach donor and acceptor to the 5′ ends of a series of double-stranded DNA oligomers of varying length. The use of DNA in such a model system has been previously shown to be valid for energy transfer measurements between organic dyes (11).

MATERIALS AND METHODS

Synthesis of Labeled DNA Oligomers. Complementary DNAs of 10, 12, and 14 bases in length were synthesized using standard phosphoramidite procedures. An amino group attached via a six-carbon linker (Glen Research, Sterling, VA) was incorporated at the 5′ end. The acceptor sequences were those used by Clegg *et al.* (11): 5′-CCACTCTAGG-3′ (10 bp); 5′-CCACTGGCTAGG-3′ (12 bp); 5′-CCACTGCTGCTAGG-3′ (14 bp). The 5-isomer of tetramethylrhodamine isothiocyanate (TMR; no. T-1480; Molecular Probes) was attached via standard procedures and purified by reverse-phase HPLC. Extinction coefficients for TMR attached to DNA were determined to be ε_{260} = 33 $mM^{-1}\cdot cm^{-1}$ and ε_{556} = 93 $mM^{-1}\cdot cm^{-1}$. The donor strand consisted of complementary DNA labeled at the 5′ end with a terbium chelate. The chelate is diethylenetriaminepentaacetic acid (DTPA) coupled to a laser dye, carbostyril 124 (cs124; see Fig. 1). Details of the donor chelate synthesis will be presented elsewhere. Unlabeled DNA oligomers were also synthesized.

Hybridization Conditions. Donor and acceptor strands were mixed in the desired ratio in a ^2H_2O-based buffer containing 10 mM Tris (pH 8.0), 10 mM $MgCl_2$, and 150 mM NaCl. Experiments were also performed in an H_2O-based buffer (data not shown). Donor strand concentration was ≈200 nM. Oligomers were annealed by heating to 75°C and cooled to the final temperature (22°C or 5°C) over 15 min.

Spectroscopy. Absorption measurements were made on a Hewlett Packard 8452A spectrometer. Steady-state fluorescence measurements were on a SPEX Fluorolog fluorimeter.

The publication costs of this article were defrayed in part by page charge payment. This article must therefore be hereby marked "*advertisement*" in accordance with 18 U.S.C. §1734 solely to indicate this fact.

Abbreviations: FRET, fluorescence resonance energy transfer; TMR, tetramethylrhodamine isothiocyanate; DTPA, diethylenetriaminepentaacetic acid; cs124, carbostyril 124.

*To whom reprint requests should be addressed.

Time-resolved and gated luminescence measurements were made on a laboratory-built spectrometer utilizing right-angle detection with a pulsed Laser-Photonics nitrogen laser (5-nsec pulse width, 40-Hz repetition rate), a gallium arsenide photon-counting detector, a gated discriminator (no. 584; Ortec, Oak Ridge, TN), and a multichannel scalar with 2-μsec time resolution (FMS board; Canberra, Schaumburg, IL). Polarization studies were also conducted, although energy-transfer experiments performed without an analyzer gave the same results as those using an analyzer. An analyzer was therefore routinely omitted. A temperature-regulated cuvette holder and a quartz 3 mm × 3 mm cuvette was used. Lifetime data was fit using TABLECURVE software (Jandel, Corte Madera, CA).

RESULTS AND DISCUSSION

Fig. 1 shows the structure of the donor chelate (DTPA-cs124-Tb) and the model system used for energy transfer. The donor chelate has several important features. First, the chelate binds terbium (and europium) extremely tightly—titration with a 100-fold excess of EDTA ($K_b \leq 10^{17}$ M^{-1}) is unable to displace a measurable amount of terbium. This is in agreement with other DTPA-based chelators (12) and ensures that there is no free terbium. Second, the chelate allows site-specific attachment of terbium to macromolecules. Third, the chelate shields the terbium from nonradiative deexcitation mechanisms, likely resulting in a quantum yield for terbium luminescence near unity in ^2H_2O (see *Quantum Yield* of *Lanthanide Emission* in *Appendix*). Finally, the covalent attachment of the laser dye cs124 overcomes the extremely low absorption cross section of terbium (<1 $M^{-1}\cdot cm^{-1}$) (6). The cs124 absorbs light (ε_{328} = 12,000 $M^{-1}\cdot cm^{-1}$; ε_{338} = 9600 $M^{-1}\cdot cm^{-1}$) and, because of its close proximity to the terbium, transfers energy to the lanthanide (13, 14).

Fig. 2 shows the spectral characteristics of the terbium chelate and the tetramethylrhodamine that lead to efficient energy transfer and a large R_o of 65 Å in ^2H_2O (60 Å in H_2O). R_o is calculated from standard equations (see *Appendix*). Here we mention two unusual aspects of using a lanthanide chelate as donor: (*i*) The efficiency of energy transfer can be adjusted, and hence R_o can be optimized for the particular system being measured, simply by varying the ratio of H_2O to ^2H_2O in the solvent. The $H_2O/^2H_2O$ ratio affects the efficiency of energy transfer by altering the lanthanide quantum yield (q_D) in our chelate ($q_D \approx 1$ in ^2H_2O; $q_D \approx 0.6$ in H_2O; see *Appendix*) (15). (*ii*) The orientation dependence of the energy transfer process is minimized because the terbium has multiple, degenerate, electronic transitions and is therefore an isotropic donor, even if stationary. This minimizes uncertainty in the measured distance due to orientation effects of ±12% in the worst case (16).

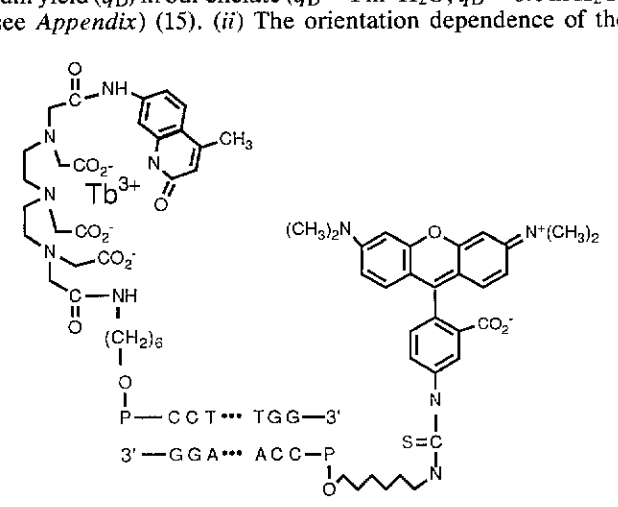

FIG. 1. Schematic diagram of double-stranded DNA with terbium chelate (donor) at one 5′ end and TMR (acceptor) at other 5′ end. In this study, the length of DNA was 10, 12, or 14 bp.

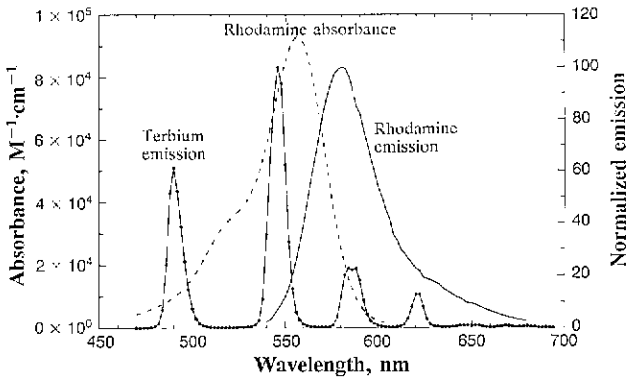

FIG. 2. Spectra of DNA labeled with either TMR or DTPA-cs124-Tb. Dashed and solid lines are the absorption and emission spectra of TMR, respectively. The solid line with circles is the emission spectrum of DTPA-cs124-Tb on DNA. The TMR emission spectrum shown was obtained on a steady-state fluorimeter. The spectral overlap between terbium emission and TMR absorption enables energy transfer to take place.

Fig. 2 also shows the highly spiked nature of the terbium emission. Donor quenching can be measured without interference from acceptor emission at 492 nm and 546 nm. Similarly, the sensitized emission of the acceptor can be measured without significant interference from donor luminescence because terbium is nearly silent around 570 nm, where TMR is at 70% of its emission maximum. The terbium signal at 570 nm is 240 times less than at its maximum, at 546 nm.

When measuring the sensitized emission, we can also eliminate the direct fluorescence of the acceptor by temporal discrimination. We use pulsed excitation and collect data only after a 90-μsec delay, during which time direct fluorescence of the rhodamine has decayed away. (The acceptor fluorescence, with a lifetime of a few nanoseconds, decays rapidly; we also find a small component—probably either delayed fluorescence or a detector artifact—which decays away within the 90-μsec delay.) The donor, because of its millisecond lifetime, stays excited and capable of transferring energy at the end of the delay period. Consequently, any signal arising around 570 nm after the delay is due only to sensitized emission (i.e., fluorescence of the acceptor due to energy transfer).

Fig. 3 shows the results of an energy transfer experiment on a partially hybridized 10-mer DNA. The *average* energy transfer in Fig. 3 is 77%. The signal-to-background ratio of the sensitized emission at 570 nm is 54:1 (see Fig. 3 legend). By comparison, the signal-to-background ratio for sensitized emission when using fluorescein–rhodamine as energy transfer pairs on the same DNA is ≈1. Because the background is so small in our case, small signals become measurable, and hence distances much greater than R_o are expected to be possible. Bruno *et al.* (6), for example, have shown the ability to measure distances of $4R_o$ (R_o = 3.1 Å) utilizing the dark-background sensitized emission of tyrosine to terbium energy transfer.

We can isolate the sensitized emission signal from donor luminescence even in regions where donor luminescence is significant. In a procedure analogous to that used by Clegg *et al.* (11), we can subtract the donor luminescence at all wavelengths, leaving the sensitized emission signal (see Fig. 3, dashed curve). The efficiency of energy transferred is then

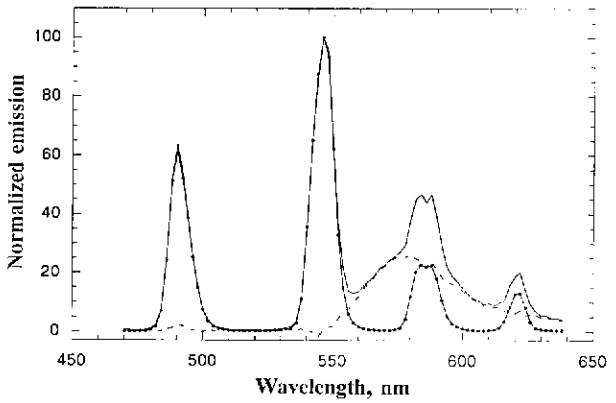

FIG. 3. Emission spectrum of a donor-only labeled double-stranded DNA (solid curve with circles), a donor–acceptor labeled double-stranded DNA (solid curve), and the difference spectra (dashed curve). The DNA length is 10 bp in all cases. The donor-only curve and donor–acceptor curves are normalized at 546 nm. In the donor–acceptor complex, the ratio of donor-strand DNA to acceptor-strand DNA is slightly greater than 1, although Fig. 4, curve C, shows that ≈12% of the donor strand is unhybridized. The signal is collected with a 7.5-msec gate after a 90-μsec delay. Data collected with a 150-μsec delay was very similar. The 54:1 signal-to-background ratio of the donor–acceptor curve at 570 nm is calculated by dividing the donor–acceptor signal at 570 nm by the donor-only signal at 570 nm. The latter is calculated by dividing the donor-only signal at 546 nm by 240. Background due to detector noise, direct acceptor fluorescence, or photon statistics are not significant. The difference spectra represent the sensitized emission. As expected, the shape is nearly identical to that of a TMR-only labeled DNA fluorescence spectrum (not shown).

simply the area of the corrected sensitized emission, divided by the total corrected area:

$$\text{efficiency of energy transfer} = (f_A/q_A)/(f_A/q_A + f_D), \quad [1]$$

where f_A is the area under the sensitized emission curve, q_A is the fluorescence quantum yield of the acceptor, and f_D is the area under the donor luminescence curve. One can determine the quantum yield of the acceptor by a comparison with the donor quenching data (Fig. 4, curve B). Based on a quantum yield of 0.174 for TMR (see *Calculating* the *Fluorescence Quantum Yield* of the *Acceptor* in *Appendix*), Eq. 1 yields an average energy transfer of 77%.

Fig. 4 shows the lifetime data on a series of DNA 10-mers. The donor-only (single-stranded DNA; curve A) signal is single exponential with a lifetime of 2.14 msec. (A terbium-labeled DNA oligomer hybridized to its complement is single exponential with a lifetime of 2.80 msec. The difference in lifetime between double-stranded and single-stranded terbium-only DNA is likely due to different radiative rates arising from different symmetries surrounding the terbium, rather than different quantum yields.) A titration with increasing amounts of acceptor strand shows biexponential donor quenching (curves B and C, Fig. 4). The long-lifetime component corresponds to unhybridized, donor-only single-stranded DNA; the short-lifetime component corresponds to those terbium strands that are hybridized with acceptor strands. As expected, increasing the amount of acceptor strand increases the amplitude of the short component and decreases the amplitude of the long component, while leaving their lifetimes unchanged (compare curves B and C). That the long-lifetime component equals the donor-only signal is an important internal control showing that intermolecular energy transfer is not significant. The lifetime of the short component corresponds to an energy transfer in the donor–acceptor complex of 88% $\left(1 - \frac{331\ \mu\text{sec}}{2809\ \mu\text{sec}}\right)$. By comparison, the

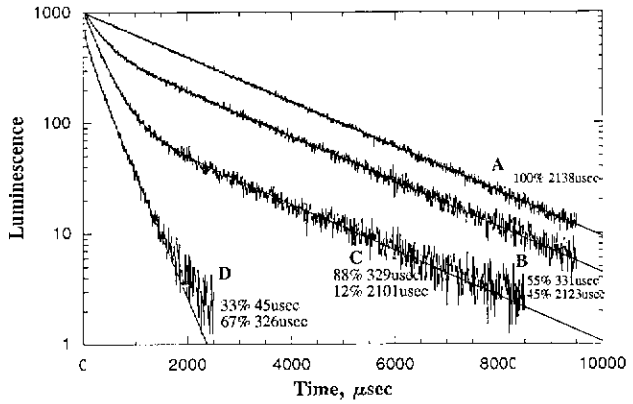

FIG. 4. Donor lifetime data at 546 nm on a donor-only labeled 10-mer single-stranded DNA (curve A), a series of partially hybridized donor–acceptor DNA 10-mers (curves B and C), and the sensitized emission signal at 570 nm (curve D) corresponding to curve B are shown. To generate curves B and C, a single-stranded donor-only DNA (curve A) was titrated with increasing amounts of acceptor-labeled complement and annealed. The solid line through each curve is a two-exponential (four parameter) fit to the data. The percentages of each component represent their amplitude; for example, curve B is fit to the equation $y = 55\% \exp(-t/331\ \mu\text{sec}) + 45\% \exp(-t/2123\ \mu\text{sec})$, indicating 55% donor–acceptor complex and 45% donor-only complex. r^2 residuals in all cases were >0.99 and for the donor-quenching curve showed no structure. Sensitized emission curve showed residual structure at >1.5 msec, possibly due to a small amount (≤1%) of signal arising from unquenched donor species. In calculating the efficiency of energy transfer based on the sensitized emission curve, we ignore the short-lifetime component, since this is due to residual signal arising from the direct fluorescence of the acceptor. (No gate was used for this data). Multiple experiments show the long-lifetime component of the sensitized emission is repeatable to within 10% in the worst case and is usually repeatable within a few percent. The short-lifetime component of the sensitized emission, however, is highly variable since there is a very large, very short spike due to direct fluorescence, which cannot be resolved.

energy transfer on the same 10-mer DNA with the same six-carbon linkers using a fluorescein–TMR pair is 23% (11).

At a 2-fold excess of acceptor strand, there is still a 10–12% unhybridized component. A similar phenomenon has been seen with dye-labeled oligomers (17) and in FRET experiments with europium substituted in our chelate (10). In our case it does not appear to be a simple melting-temperature phenomenon since it is present at both 5°C and 22°C. The reason for this is unknown, although it is possible that some fraction of the synthetic donor-strand DNA was not fully deprotected and hence was unable to hybridize. (The amide linkage between DTPA and cs124 is base-labile and so mild deprotection must be used.) It is unlikely that this residual unquenched donor signal is due to fundamental lanthanide photophysics since this would require an uncoupled magnetic dipole transition, a situation that is not present since all terbium (and europium) luminescence arises from the same excited state (18, 19).

Fig. 4 also shows the lifetime of the sensitized emission at 570 nm corresponding to the biexponential donor quenching (curve B). The sensitized emission decay can be accurately fit to the equation $y = 33\% \exp(-t/45\ \mu\text{sec}) + 67\% \exp(-t/326\ \mu\text{sec})$. The 45-μsec component corresponds to direct fluorescence from the acceptor or a detector artifact (which can be eliminated by gating). The 326-μsec component is due to energy transfer on the donor–acceptor complex and agrees extremely well with the 329- to 331-μsec donor quenching component. Note that after ≈90 μsec, the only species that contribute to the sensitized emission signal is the donor–acceptor complex—donor-only or acceptor-only do not contribute. This significantly minimizes the problem of incom-

Table 1. Comparison of energy transfer and distances on DNA duplexes in this work and in ref. 11

DNA duplex	Lifetime, μsec	Efficiency of energy transfer	Distance, Å	
			This work	Ref. 11
10-mer	336	0.88	46.6	55.5
12-mer	724	0.74	54.6	56.4
14-mer	1154	0.59	61.2	61.0

Both results are consistent with the DNA double-helix geometry, although differing salt conditions and donor lifetimes lead to different dye positions and hence different measured distances.

plete labeling. The sensitized-emission lifetime signal is also insensitive to total concentration, to quantum yields, and to non-energy-transfer effects, which can cause donor quenching.

In Table 1 we summarize lifetime and energy transfer data on donor–acceptor-labeled DNA duplexes of 10, 12, and 14 bp in length. Data from multiple experiments show that donor quenching and sensitized emission lifetimes for a given length of DNA always agree within 10% and usually agree within a few percent. As expected, there is a decrease in energy transfer with increasing distance. For comparison we include the distances determined by Clegg *et al.* (11) using fluorescein–TMR. We have fit our distances using the Clegg *et al.* model of the DNA helix and attached dyes. With only three data points, it is not possible to resolve uniquely all the parameters in the model, but, nevertheless, a good fit to their model is achieved if it is assumed that the terbium chelate and/or acceptor are fairly close to the DNA helix. This reduces the modulation seen in their FRET data, which arises because of the helical geometry of the DNA and the fact that their donor and acceptor are extended away from the helix (19 Å and 13 Å, respectively). This difference is qualitatively reasonable since the long lifetime of our donor is expected to allow constrained diffusion of the donor and acceptor within the limits placed by the six-carbon linkers and because of the greater ionic strength used here, which minimizes charge repulsion.

In summary, the data are consistent with the geometry of the double-helix DNA if the energy transfer data are derived based on the dipole–dipole Förster-type mechanism. Numerous technical advantages of luminescence resonance energy transfer make this a technique well suited for measurements on biologically interesting macromolecules.

APPENDIX

Calculation of R_o. R_o, the distance at which 50% of the donor's excited state energy is transferred to the acceptor, is calculated from standard equations (1):

$$R_o = (8.79 \times 10^{-5}\, J\kappa^2 n^{-4} q_D)^{1/6}\ \text{Å}, \qquad [2]$$

where q_D is the luminescence quantum yield for donor emission in the absence of acceptor, J is the spectral overlap of the donor emission (f_D) and acceptor absorption (ε_A) ($J = \int\int f_D \varepsilon_A \lambda^4 d\lambda$), n is the index of refraction, and κ^2 is a geometric factor related to the relative angles of the two dipoles. Here we evaluate each of the terms in Eq. **2** and discuss their uncertainty.

The index of refraction, n, varies from 1.33 for water to 1.39 for many organic molecules. We have used 1.33. A numerical integration leads to a J overlap integral of 3.8×10^{15} $nm^4 \cdot M^{-1}$. This is an upper limit for J since the 546-nm peak of terbium may arise from magnetic dipole, as well as electric dipole transitions (19), and the former do not significantly transfer energy (18). The fraction of magnetic dipole contribution can be calculated theoretically (20, 21), or the problem can be avoided by using the 492-nm line of terbium, which is known to be solely an electric dipole transition (20).

When using organic dyes in FRET, κ^2 is often a significant source of uncertainty and, in the worst case, may vary from 0 to 4 (22). With terbium, however, emission arises from multiple electronic transitions that constrain κ^2: $1/3 < \kappa^2 < 4/3$. In addition, it is likely that the acceptor can undergo rotational motion during the millisecond donor lifetime. This further constrains κ^2, and we assume $\kappa^2 = 2/3$, corresponding to a random orientation rotating rapidly within the donor lifetime.

The luminescence quantum yield of the terbium, q_D, is difficult to accurately determine because of terbium's intrinsically low absorbance. q_D, however, is likely very close to 1 in ^2H_2O (see below). Note that when calculating R_o, it is important to use the terbium quantum yield ($\approx$1 in ^2H_2O), not the quantum yield of the entire chelate. The quantum yield of the entire chelate equals the lanthanide quantum yield times the fraction of energy absorbed by the cs124 that is transferred to the lanthanide.

Quantum Yield of Lanthanide Emission. There are several lines of (indirect) evidence that argue that $q_D \approx 1$ in ^2H_2O. First, emission arises from 4f–4f inner shell electrons, which are shielded from the solvent and other sources of nonradiative deexcitation by the chelate. The 1.2 H_2O molecules in the primary coordination sphere of the terbium in our chelate (data not shown) are the primary source of nonradiative deexcitation, but these are replaced by ^2H_2O, which do not significantly deactivate terbium (15, 23). The nonwater ligands, carboxylate groups, and amine nitrogens are extremely inefficient at deactivating the terbium excited state (23). Via temperature studies (24), we have also looked for quenching effects of the cs124 and have found none (data not shown).

A second line of evidence supporting $q_D \approx 1$ in ^2H_2O comes from the work of Elbanowski *et al.* (25), who directly measured the quantum yield of a 1:3 mixture of terbium/EDTA in H_2O and found a value of 0.54. This measurement is difficult and of unknown accuracy, but, nevertheless, it suggests a high quantum yield even in H_2O, and the quantum yield in ^2H_2O is expected to be considerably higher. [There are probably 2 water molecules coordinated to the terbium in their complex (23)].

The third line of evidence comes from energy transfer experiments using terbium as a donor in thermolysin (8, 26) and as an acceptor in invertebrate calmodulin (6), where the assumption (sometime implicit) of unity quantum yield in ^2H_2O gives good agreement with x-ray crystallography data.

Calculating the Fluorescence Quantum Yield of the Acceptor. By comparing the donor quenching lifetime data (curve C in Fig. 4) with the areas in Fig. 3 and using Eq. **1**, it is possible to measure the quantum yield of the acceptor. This is a general and new method for measuring quantum yields of any dye whose absorption overlaps the emission of terbium (or europium). It has the advantage over more conventional methods of measuring quantum yields in that the measurement involves only one sample—the actual sample of interest—rather than comparing a reference to the sample.

To evaluate the quantum yield of TMR, we assume the unknown in Eq. **1** is q_A and take the average efficiency of energy transfer to be 77.6%, as determined from curve C of Fig. 4. Based on the integrated areas (620 for f_A and 1032 for f_D, in arbitrary units), this yields $q_A = 0.174$. By comparison, free tetramethylrhodamine in phosphate-buffered saline has a quantum yield of 0.28, as measured by standard techniques (27).

We thank Mel Klein, Tom Jovin, and Bob Clegg for stimulating discussions and Lynn Myers of the Midland Certified Reagent Company for excellent technical assistance in the preparation of rhodamine-labeled oligomers. This work was supported by National

Institutes of Health Grant R01 GM 41911 and by the Office of Energy Research, Office of Health and Environmental Research of the Department of Energy, under contract DE AC03-76SF00098.

1. Cantor, C. R. & Schimmel, P. R. (1980) *Biophysical Chemistry* (Freeman, San Francisco).
2. Clegg, R. M. (1992) *Methods Enzymol.* **211,** 353–388.
3. Selvin, P. R. (1994) *Methods Enzymol.* **246,** in press.
4. Van Der Meer, B. W., Coker, G., III, & Chen, S. Y. (1994) *Resonance Energy Transfer* (VCH, New York).
5. Stryer, L., Thomas, D. D. & Meares, C. F. (1982) *Annu. Rev. Biophys. Bioeng.* **11,** 203–222.
6. Bruno, J., Horrocks, W. D., Jr., & Zauhar, R. J. (1992) *Biochemistry* **31,** 7016–7026.
7. Cronce, D. T. & Horrocks, W. D., Jr. (1992) *Biochemistry* **31,** 7963–7969.
8. Horrocks, W. D., Jr., Holmquist, B. & Vallee, B. L. (1975) *Proc. Natl. Acad. Sci. USA* **72,** 4764–4768.
9. Mathis, G. (1993) *Clin. Chem.* **39,** 1953–1959.
10. Selvin, P. R., Rana, T. M. & Hearst, J. E. (1994) *J. Am. Chem. Soc.* **116,** 6029–6030.
11. Clegg, R. M., Murchie, A. I., Zechel, A. & Lilley, D. M. (1993) *Proc. Natl. Acad. Sci. USA* **90,** 2994–2998.
12. Oser, A., Collasius, M. & Valet, G. (1990) *Anal. Biochem.* **191,** 295–301.
13. Abusaleh, A. & Meares, C. (1984) *Photochem. Photobiol.* **39,** 763–769.
14. Kirk, W. R., Wessels, W. S. & Prendergast, F. G. (1993) *J. Phys. Chem.* **97,** 10326–10340.
15. Horrocks, W. D., Jr., Schmidt, G. F., Sudnick, D. R., Kittrell, C. & Bernheim, R. A. (1977) *J. Am. Chem. Soc.* **99,** 2378–2380.
16. Stryer, L. (1978) *Annu. Rev. Biochem.* **47,** 819–846.
17. Cooper, J. P. & Hagerman, P. J. (1990) *Biochemistry* **29,** 9261–9268.
18. Dexter, D. L. (1953) *J. Chem. Phys.* **21,** 836–850.
19. Bunzli, J.-C. G. (1989) in *Lanthanide Probes in Life, Chemical and Earth Sciences*, eds. Bunzli, J.-C. G. & Choppin, G. R. (Elsevier, New York), pp. 219–293.
20. Carnall, W. T., Fields, P. R. & Rajnak, K. (1968) *J. Chem. Phys.* **49,** 4412–4423.
21. Gorller-Walrand, C., Fluyt, L., Ceulemans, A. & Carnall, W. T. (1991) *J. Phys. Chem.* **95,** 3099–3106.
22. Dale, R. E., Eisinger, J. & Blumberg, W. E. (1979) *Biophys. J.* **26,** 161–194.
23. Horrocks, W. D., Jr., & Sudnick, D. R. (1979) *J. Am. Chem. Soc.* **101,** 334–350.
24. Alpha, B., Ballardini, R., Balzani, V., Lehn, J.-M., Perathoner, S. & Sabbatini, N. (1990) *Photochem. Photobiol.* **52,** 299–306.
25. Elbanowski, M., Lis, S. & Konarski, J. (1989) *Monat. Chem.* **120,** 699–703.
26. Berner, V. G., Darnall, D. W. & Birnbaum, E. R. (1975) *Biochem. Biophys. Res. Commun.* **66,** 763–768.
27. Haugland, R. P. (1983) in *Excited States of Biopolymers*, ed. Steiner, R. F. (Plenum, New York), pp. 29–58.